

## Electronic Supplementary Information

### Solvent-Driven Migration of Highly Polar Monomers into Hydrophobic PDMS Produces Thick Graft Layer via Subsurface Initiated ATRP for Efficient Antibiofouling

Xin Yu,<sup>a</sup> Yang Yang,<sup>b</sup> Wufang Yang,<sup>c</sup> Xungai Wang,<sup>a</sup> Xin Liu,<sup>\*,a</sup> Feng Zhou<sup>\*,c</sup> and Yan  
Zhao<sup>\*,d</sup>

<sup>a</sup> Institute for Frontier Materials, Deakin University, Geelong, Victoria 3216, Australia

<sup>b</sup> College of Textiles, Donghua University, Shanghai 201620, China

<sup>c</sup> State Key Laboratory of Solid Lubrication, Lanzhou Institute of Chemical Physics, Chinese  
Academy of Sciences, Lanzhou 730000, China

<sup>d</sup> College of Textile and Clothing Engineering, Soochow University, Suzhou 215123, China

\*Xin Liu. Email: xin.liu@deakin.edu.au;

\*Feng Zhou. Email: zhouf@licp.cas.cn;

\*Yan Zhao. Email: yanzhao@suda.edu.cn.

## EXPERIMENTAL SECTION

### Materials

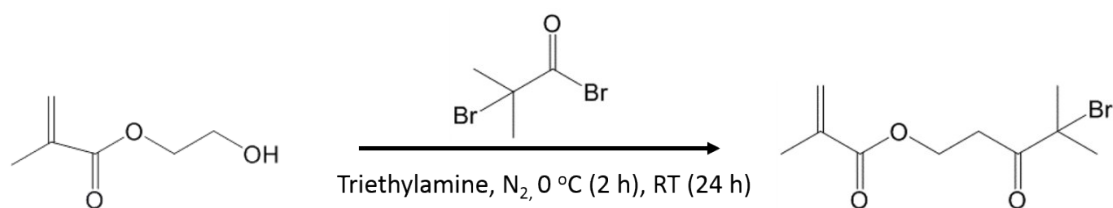
Poly(dimethylsiloxane) (Sylgard 184) was purchased from Dow Corning. 2-Hydroxyethyl methacrylate (HEMA, 99%), triethylamine (99%), 2-(dimethylamino)ethyl methacrylate (DMAEMA), 1-bromoundecane (98%), cuprous bromide (CuBr, 98%),  $\alpha$ -bromoisobutyryl bromide (BIBB, 98%), 2,2'-bipyridyl (BPY, 99%), dopamine hydrochloride (DOPA), methacrylic anhydride (94 %), azobisisobutyronitrile (AIBN, 0.2 M in toluene) and 3-sulfopropyl methacrylate potassium salt (SPMA) were purchased from Sigma-Aldrich. N-(3-Sulfopropyl)-N-(methacryloxyethyl)-N,N-dimethylammoniumbetaine (SBMA, 97%) was purchased from Merck. Hydrochloric acid (AR, 37%), methanol (MeOH, AR), tetrahydrofuran (THF, AR), isopropyl alcohol (IPA, AR), acetonitrile (AR), dichloromethane (CH<sub>2</sub>Cl<sub>2</sub>, AR), sodium chloride (NaCl), sodium bicarbonate (NaHCO<sub>3</sub>), and magnesium sulfate (MgSO<sub>4</sub>) were purchased from Chem-Supply Pty Ltd (Australia). Anhydrous dichloromethane and anhydrous triethylamine were obtained by adding a small amount of calcium hydride (CaH<sub>2</sub>) and then distilled under vacuum condition. CuBr was purified by stirring in acetic acid for 3 h and washing with ethanol as well as diethyl ether, and then dried in vacuum oven at 40 °C prior to being stored in a vacuum desiccator.

Fluorescein isothiocyanate-label bovine serum albumin (FITC-BSA), phosphate buffered saline (PBS, one tablet dissolved in 200 mL of DI water yields 0.01 M phosphate buffer, 137 mM sodium chloride, and 2.7 mM potassium chloride, pH 7.4 at 25 °C) and sodium dodecyl sulfate (SDS) were purchased from Sigma-Aldrich and used without further purification. Solution for the static protein adsorption assay was prepared by dissolving BSA in 20 mL PBS solution with different concentrations. Protein contents were determined using a bicinchoninic acid (BCA) assay kit from Pierce, no. 23235 (Thermo Fisher Scientific, Inc.

USA) according to the vendor's protocol. Deionized (DI) water (18 M $\Omega$ ) produced with a Milli-Q system was used in the study.

### Synthesis of 2-(2-bromoisobutyryloxy) ethyl methacrylate (BIEM)

Bromide-containing initiator was synthesized according to a reported method (Scheme 1).<sup>1,2</sup> Briefly, a 100 mL three neck flask containing 20 mL of dry CH<sub>2</sub>Cl<sub>2</sub>, 1.314 g (10 mmol) of 2-hydroxyethyl methacrylate (HEMA), and 1.214 g (12 mmol) of triethylamine was equipped with stir bar and cooled to 0 °C in an ice bath. Using an additional funnel, 2.759 g (12 mmol) of 2-bromoisobutyryl bromide (BIBB) was added dropwise into the flask over 2 h. Upon complete addition, the mixture was stabilized at room temperature and stirred for 24 h. The precipitation was filtered and the clear organic layer was washed with 2 M HCl, saturated NaHCO<sub>3</sub>, and saturated NaCl solution, respectively, to obtain organic solution via separating funnel. The separated solution was dried over anhydrous MgSO<sub>4</sub>, and the solvent was evaporated. The remaining pale yellow oil was collected. The desired product (BIEM) was confirmed by <sup>1</sup>H NMR (CDCl<sub>3</sub>)  $\delta$ : 6.14 (s, 1H); 5.60 (s, 1H); 4.39 (m, 4 H); 1.94 (s, 3 H); 1.93 (s, 6H).



**Scheme S1** Synthesis of initiator 2-(2-bromoisobutyryloxy) ethyl methacrylate.

### Preparation of PDMS and iPDMS

PDMS was prepared by mixing the precursor (A) and curing agent (B) at a weight ratio of 10:1, followed by curing at 100 °C for 4 h. To prepare iPDMS, the vinyl-terminated alkyl bromine initiator BIEM was mixed well with the PDMS precursor (A) and curing agent (B). The weight ratio of initiator BIEM to PDMS was set to be 0.1, 0.25, 0.5, 0.75, and 1, respectively. This

mixture was then poured into a glass petri dish and cured at 100 °C for 4 h. Then, a transparent elastomer was obtained and cut into desired size for further surface modification. It is noted that the carbon-carbon double bond of initiator could react with hydrosilane hydrogen in the presence of Pt catalysts, resulting in a highly cross-linked three dimensional network.

### **Preparation of PSBMA brushes via SSI-ATRP**

Before surface grafting, all PDMS and iPDMS samples were immersed in hexane for 24 h to remove any physisorbed and entrapped initiator. The swollen samples were dried under N<sub>2</sub> flow for further surface grafting. For surface grafting of hydrophilic zwitterionic monomer, different organic solvents (THF, IPA, and MeOH) mixed with water at different ratios were used for surface grafting. Specifically, SBMA (3 g, 10 mmol) was then dissolved in 6 mL one of water-organic binary solvents and the solution was degassed with dry N<sub>2</sub> for 30 min under stirring. Then, 31.2 mg of BPY (0.2 mmol) and 14.6 mg of CuBr (0.1 mmol) was added into the solution, respectively, to form a clear solution under stirring. Then the solution was syringed into a Schlenk flask, where PDMS or iPDMS was sealed with N<sub>2</sub> protection. After polymerization, the samples were collected and washed with 0.1 M NaCl (at 60 °C) and water thoroughly to remove the monomer, solvent, and homopolymerized PSBMA. The samples were dried under N<sub>2</sub> flow for further characterizations.

The procedure for poly(3-sulfopropyl methacrylate potassium salt) (PSPMA) was similar. Reaction conditions were as follows: SPMA (2.5 g, 10 mmol), CuBr (14.6 mg, 0.1 mmol), BPY (31.2 mg, 0.2 mmol), (THF/H<sub>2</sub>O=1:5, MeOH/H<sub>2</sub>O=9:1, IPA/H<sub>2</sub>O=2:1), 12 h.

### **Characterizations**

Static water contact angle (WCA) of polymer grafted PDMS was determined by the sessile drop method using a CAM 101 video camera based contact angle measurement system (KSV Instruments Ltd., Finland). Fourier transform infrared (FTIR) spectra were recorded on Bruker VERTEX 70 instrument using attenuated total reflectance (ATR) mode with a resolution of 4

cm<sup>-1</sup> accumulating 32 scans. Lumos ATR-FTIR (Bruker, USA) with huge field of view and visual resolution in the sub micrometer range was used to characterize the distribution of monomer from surface to subsurface. <sup>1</sup>H nuclear magnetic resonance (NMR) spectrum was recorded on a Bruker AVANCE 500 MHz NMR spectrometer and chloroform-d (CDCl<sub>3</sub>) was used as solvent. X-ray photoelectron spectroscopy (XPS) measurement was performed with a Thermo Scientific K-Alpha XPS system. X-ray source was a monochromatized Al K $\alpha$  radiation (h $\nu$ =1486.6 eV). Three different sites on per sample were measured. Each measurement contains a survey scan and a high resolution measurement for main elements. Surface morphology and cross-section were observed using a Supra 55 VP scanning electron microscope (SEM) operated at an acceleration voltage of 5 kV. Energy dispersive X-ray (EDX) analysis was undertaken on Supra 55 VP with integrated EDX detector. Atomic force microscopy (AFM) was conducted with a Bruker MultiModel 8 SPM instrument (Bruker, USA) using the tapping model. For the tensile test, dog-bone shaped specimens were prepared. Briefly, the precursor (A) and curing agent (B) at a weight of 10: 1 with different ratios of initiator BIEM (0.1, 0.25, 0.5, 0.75, and 1) were mixed very well before pouring into PTFE mould, which has same gauge length (20 mm), thickness (3 mm), and width (4 mm). Six specimens were cured at 100 °C for 10 h and tested under room temperature for each group and results were averaged for analysis.

The swelling ratio of iPDMS in different solvents were characterized by comparing the weight difference before and after soaking. Pre-weighted dry iPDMS samples were immersed in various solvents at room temperature. Then, the samples were weighed after the removal of excessive surface solvent by filter paper. The swelling ratio at different time can be calculated from the following equation.

$$\text{Swelling ratio (\%)} = [(W_s - W_d)/W_d] \times 100$$

where  $W_s$  represents the weight in the swollen state of a sample at a given time and  $W_d$  is the weight of the dry sample. Each experiment was repeated three times.

### **Protein adsorption test**

BSA protein was selected as a model protein for adsorption test. Prior to adsorption, pristine PDMS and polymer coated PDMS were immersed in PBS solution overnight. Then, 2 mL FITC-BSA (0.1 mg/mL) was added into vials containing samples. The vials were kept in dark for 24 h at 37°C. After adsorption, the samples were rinsed with fresh PBS solution five times to remove the non-adhered FITC-BSA protein. The FITC-BSA adsorbed onto substrates was detected using a fluorescence microscope (Zeiss Microscope, Primovert iLED, magnification 40X). The strategy for quantifying FITC-BSA adsorption was to calculate the mean grey value of image by Image J (National Institutes of Health, USA) because the grey value is proportional to the amount of fluorescent labelled protein adsorbed on the surface. Fluorescence intensity of PSBMA coated samples was normalized relative to the intensity of FITC adsorbed on iPDMS to make the comparison systematic. The mean grey value of the samples before exposure to FITC-BSA was used as background and it was subtracted prior to normalization.

### **Bacteria adhesion test**

As for bacteria adhesion test, *E.coli* was selected as a representative microorganism to evaluate the antibiofouling abilities of iPDMS-PSBMA. Prior to adhesion, the pristine and modified PDMS substrates were sterilized by UV irradiation for 1 h and then immersed in 20 mL bacterial suspension of  $10^7$  CFU/mL in a sterile Erlenmeyer flask for 24 h at 37 °C. After that, each sample was taken out and rinsed 3 times with sterile PBS. Bacteria adhered to the PDMS surface were fixed with 2.5 vol. % glutaraldehyde in PBS (1 mL 25 % glutaraldehyde, 9 mL 0.01 M PBS) at 4 °C for 4 h. Finally, the sample was washed several times with sterilized PBS, and dehydrated with a series of ethanol/water mixtures (30, 50, 70, 85, 90 vol. % ethanol; 15 min for each step). The dried PDMS surface was then observed by SEM. Quantitative data

about the density of adhered bacteria was calculated from SEM images and each value is the average of six areas on one sample.

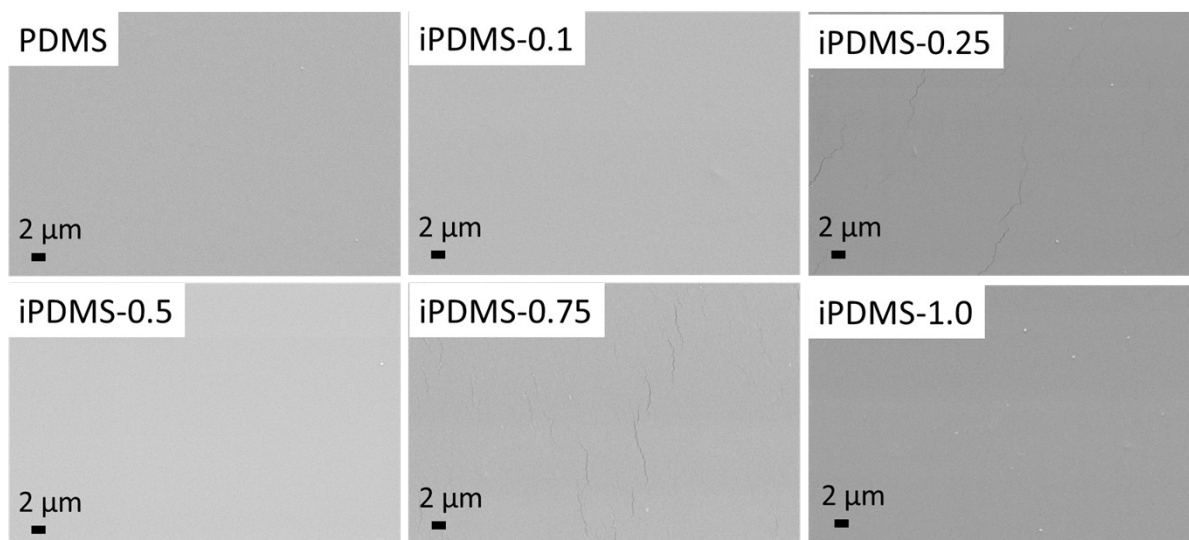


**Fig. S1** Surface morphology of PDMS and iPDMS with different initiator contents.

The surface morphology was investigated at different weight ratios of initiator (0.1wt%, 0.25wt%, 0.5wt%, 0.75wt%, and 1wt%). Results showed that there was no distinguishable difference between the surface morphology of pristine PDMS and initiator-embedded PDMS.





**Fig. S2** Water contact angle of PDMS and iPDMS with different initiator contents.

The slight decrease in water contact angle indicates the presence of hydrophilic initiator molecules on PDMS surface.

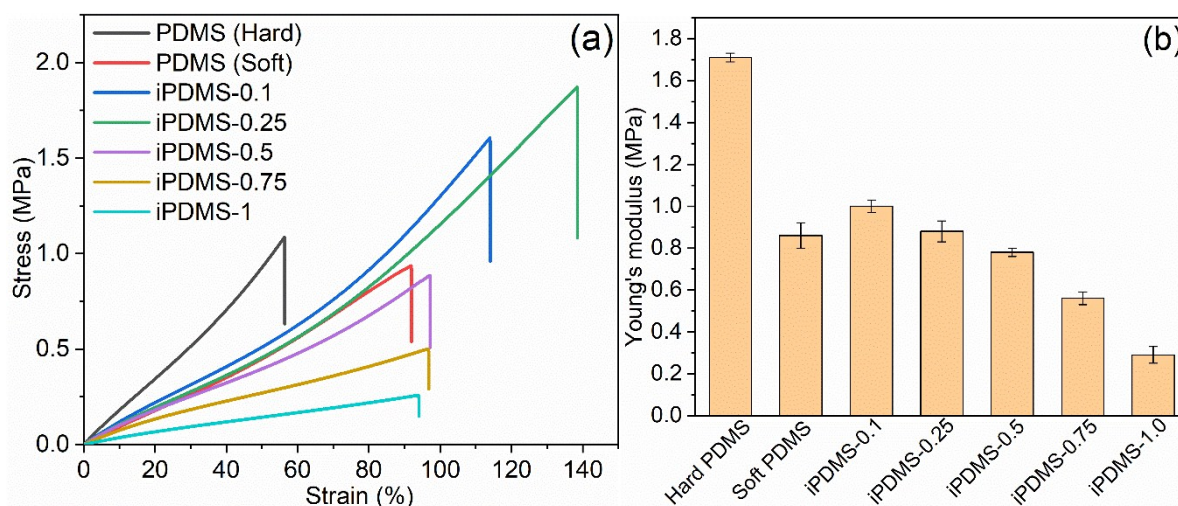


**Fig. S3** (a) Stress-strain curves and (b) Young's modulus of PDMS and iPDMS samples with different initiator contents.

The mechanical property of initiator-embedded PDMS was dependent on the initiator content (Fig. S3a). Long curing time (10 h) of pristine PDMS resulted in high strength but low elongation (Hard PDMS). However, the strain increased significantly when initiator was introduced in PDMS. When the initiator content was 0.25wt% (iPDMS-0.25), the strain reached ~140%. However, the strain decreased dramatically with further increasing the initiator content. This is because the presence of excess initiator disturbs the cross-linking of PDMS significantly. As a result, not only the stress but also the strain became lower when the initiator content exceeded the critical value of 0.25wt%. In real applications, especially for biomaterials and microfluidic system, soft PDMS with good flexibility is promising.<sup>3,4</sup> As we know, long curing time promotes the cross-linking, which results in high strength but low elongation.<sup>5</sup> So we reduced the curing time to 1 h for PDMS without initiator. As shown in Fig. S4a, the PDMS had good elongation as well as strength, and it was denoted as soft PDMS. In addition, the Young's modulus was calculated for the linear elastic region (<40 % strain) using Hooke's law<sup>6</sup> as shown in Fig. S3b. It can be seen that the Young's modulus decreased obviously with the increase of initiator content. However, in comparison to PDMS with low curing time (1 h),

iPDMS showed comparable Young's modulus when the initiator content was less than 0.5wt%. As a result, iPDMS-0.5 showed good performance from the viewpoint of not only the strength but also the flexibility and it was selected as substrate for SSI-ATRP in this work.

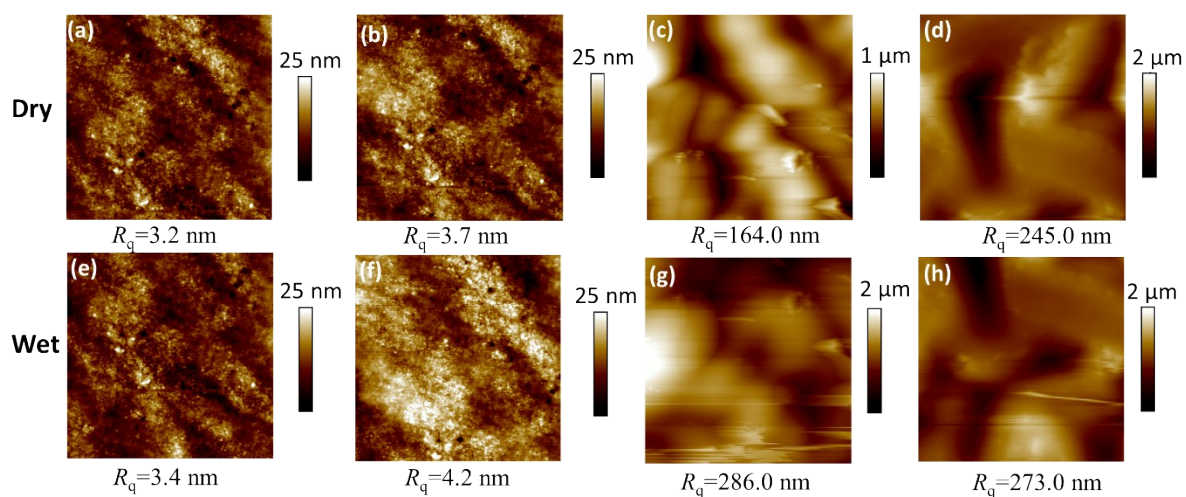


**Fig. S4** AFM images in dry and wet states: (a, e) iPDMS and PSBMA-grafted PDMS using binary solvent (b, f) THF:H<sub>2</sub>O=1:1, (c, g) IPA:H<sub>2</sub>O=3:1, and (d, h) MeOH:H<sub>2</sub>O=9:1.

The surface of iPDMS is smooth and the root-mean-square roughness ( $R_q$ ) is 3.2 nm. After grafting, the  $R_q$  is 3.7 nm for the case of THF-water binary solvent, while the  $R_q$  is quite large for the cases of IPA-water and MeOH-water solvents. When the sample was in wet state, the  $R_q$  is a bit larger than that of the same sample in dry state due to the swelling of PSBMA polymer chains in water.

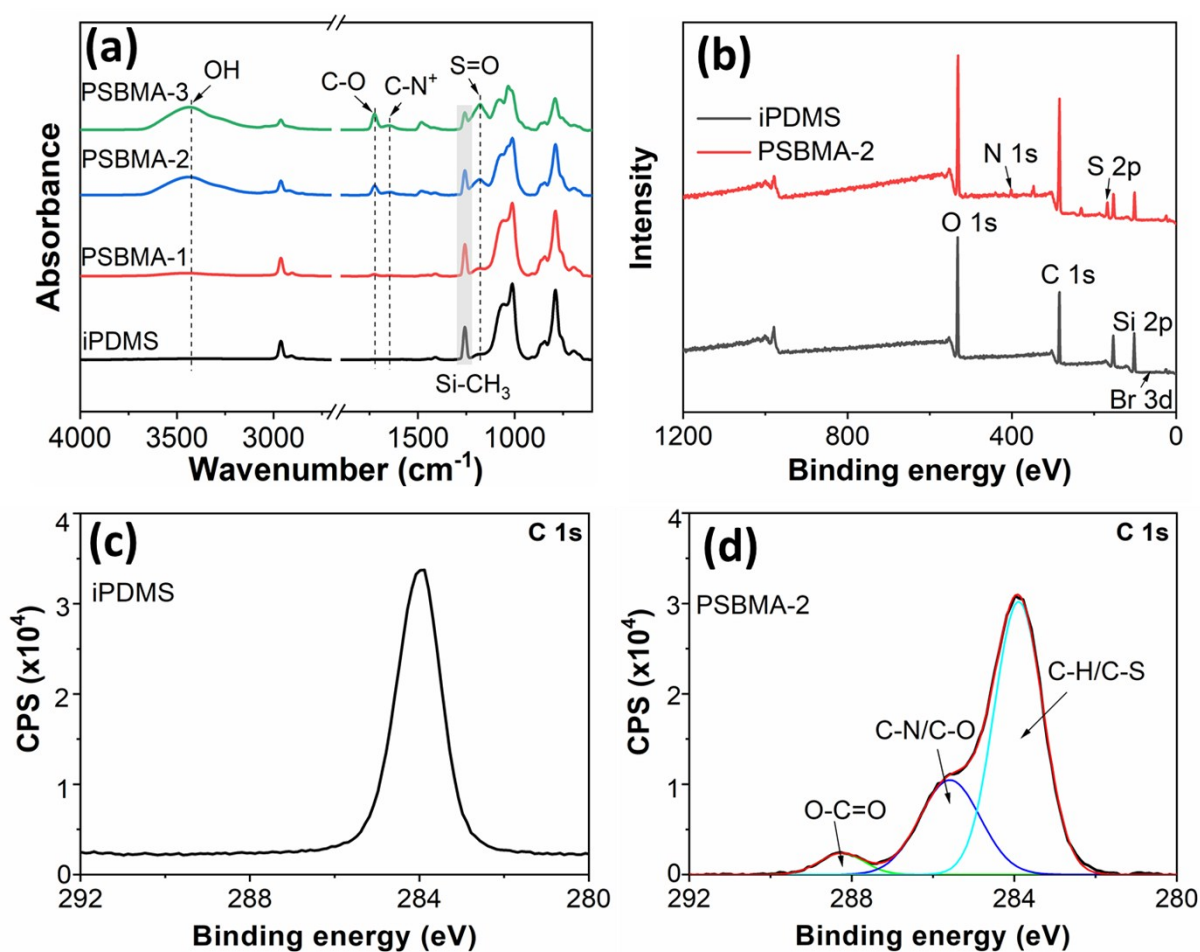


**Fig. S5** (a) ATR-FTIR spectra, (b) XPS survey scan, and (c, d) C 1s high resolution scan of iPDMS and PSBMA grafted PDMS. PSBMA-1, PSBMA-2, and PSBMA-3 represents the sample prepared using isopropyl alcohol and water mixture at a ratio of 1:1, 2:1, and 3:1, respectively.

Fig. S5a shows the ATR-FTIR spectra of iPDMS and PSBMA grafted PDMS using binary solvent containing IPA and water. For iPDMS, a peak appeared at 1250 cm<sup>-1</sup> because of Si-CH<sub>3</sub> stretching vibration. After PSBMA grafting, distinctive peaks appeared at 1726 cm<sup>-1</sup> due to the stretching vibration of C=O from ester group, as well as at 1644 cm<sup>-1</sup> and 1180 cm<sup>-1</sup> as a result of C-N<sup>+</sup> and S=O stretching, respectively. A broad absorption at the center of 3450 cm<sup>-1</sup> appeared due to the adsorbed water from the atmosphere via ionic solvation of PSBMA. Furthermore, the intensity of these peaks increased with the increase of IPA volume fraction due to the higher grafting density of PSBMA (Fig. 1e, 1g, and 1h). XPS measurement was also

conducted to verify the presence of PSBMA. As shown in Fig. S5b, survey scan of iPDMS shows the characteristic peaks of PDMS. After PSBMA grafting, peaks of S 2p (167.4 eV) and N 1s (402.1 eV) are detected. The high-resolution C 1s spectrum of iPDMS is shown in Fig. S5c. A peak assigned to C-H (~285.0 eV) can be observed. After PSBMA grafting, there appeared peaks at 288.3, 285.6 and 284.0 eV that can be ascribed to O-C=O, C-O/C-N, and C-S/C-H, respectively, indicating the presence of PSBMA on PDMS surface (Fig. S5d).

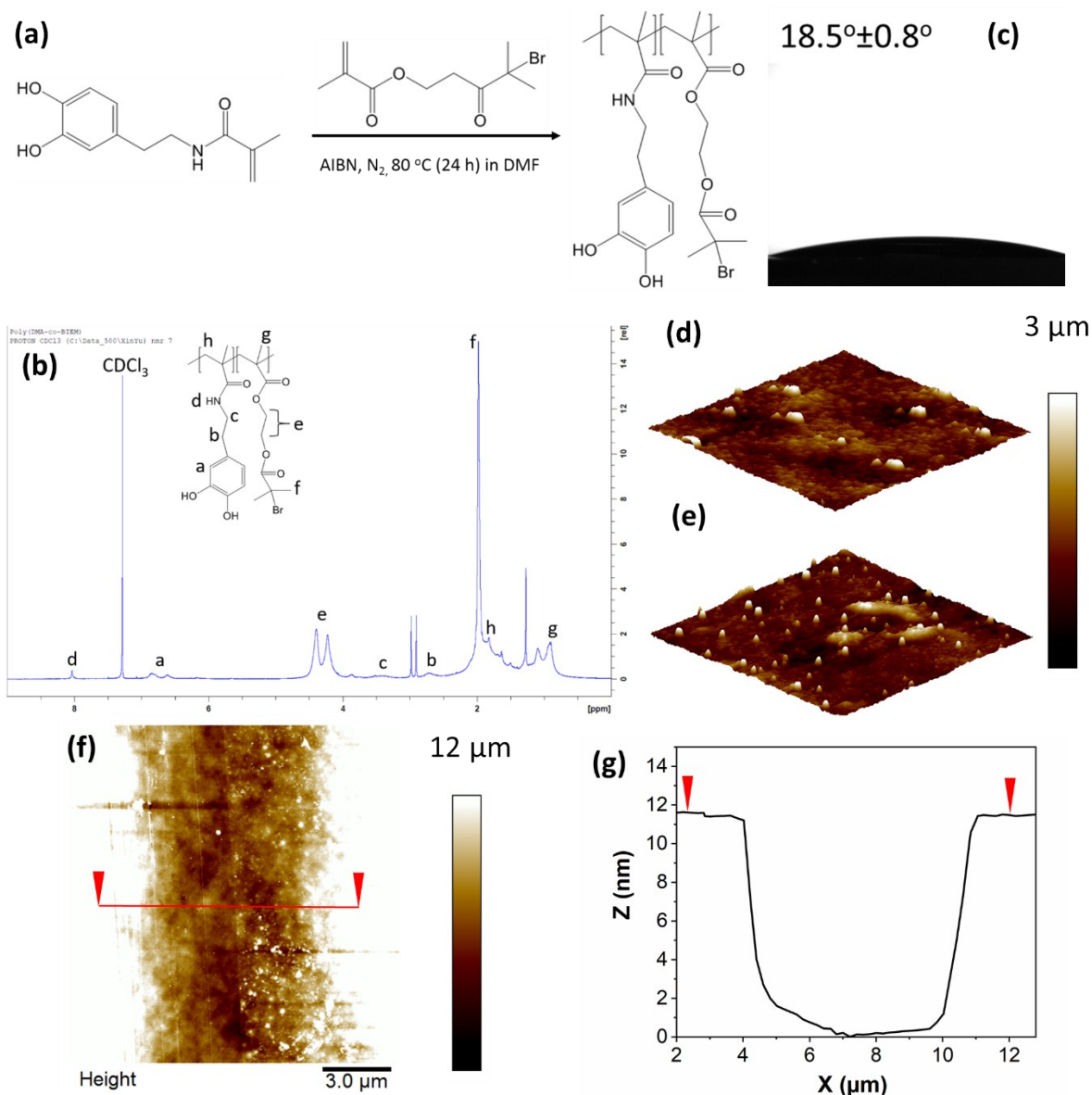


**Fig. S6** (a) Synthesis of dopamine modified initiator and (b)  $^1H$  NMR spectrum of initiator; (c) water contact angle of PSBMA-grafted silicon wafer via SI-ATRIP; (d) AFM 3D images of iPDMS and (e) PSBMA-grafted silicon wafer; (f) AFM images of PSBMA-grafted silicon wafer after scratching (top-down); (g) height profile (Z-axis) of red line (X-axis) according to AFM step-height analysis.

A dopamine modified initiator (Fig. S6a) was synthesized via free radical polymerization (dopamine methacrylate:BIEM=2:8, mol:mol) and confirmed by  $^1H$  NMR (Fig. S6b). Then, the initiator was immobilized onto plasma activated silicon wafer and it was polymerized under

the same condition with iPDMS using a ratio of IPA to water at 2:1. After grafting, a low water contact angle indicates the successful grafting of zwitterionic polymer brushes (Fig. S6c). The root-mean-square roughness ( $R_q$ ) of initiator immobilized surface (Fig. S6d) and PSBMA-grafted silicon wafer (Fig. S6e) are 0.368 nm, and 0.571 nm, respectively, for a  $1\ \mu\text{m} \times 1\ \mu\text{m}$  scan area. There is no distinct change in surface morphology and roughness after surface grafting, indicating the PSBMA polymer brushes are smooth and highly uniform. In addition, we can evaluate the thickness of polymer brushes using step-height analysis in AFM.<sup>7-9</sup> A slight scratch was made on the PSBMA-grafted silicon wafer surface and the tip was carefully located at the edge of the scratch before scanning (Fig. S6f). Fig. S6g shows the thickness of PSBMA polymer brushes was about  $11.5 \pm 1.5\ \text{nm}$ , which is consistent to the results in previous reports.<sup>7, 10</sup> However, it should be noted that the film thickness is lower than some other reports.<sup>11, 12</sup> This may be attributed to the lower density of dopamine modified initiator on silicon wafer than silane-based initiator.



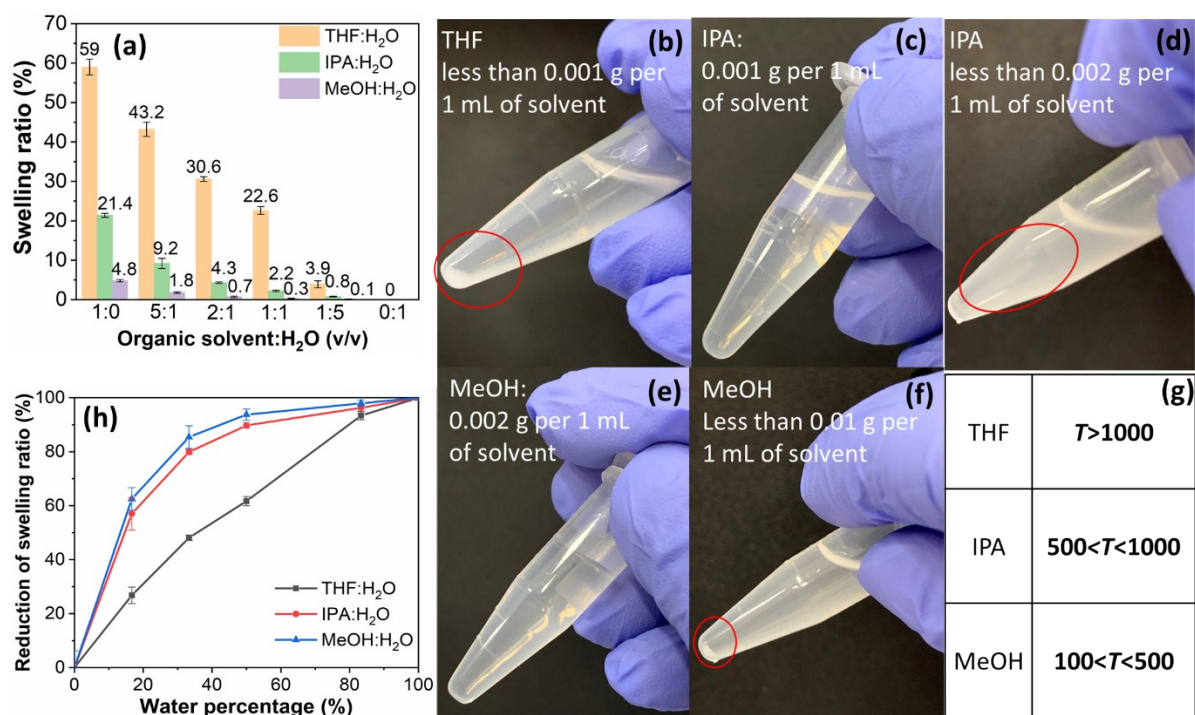


**Fig. S7** (a) Swelling ratio of iPDMS in different organic solvent and water mixtures at various ratios. (b-f) Images of zwitterionic monomer SBMA dissolving in pure organic solvents. (g) Threshold ( $T$ ). (h) Reduction of swelling ratio along with the volume ratio of water.

The threshold ( $T$ ) is defined as mass parts of solvent required to dissolve 1 mass part of solute.<sup>13</sup> As shown in Fig. S7b, the threshold of THF is larger than 1000 since 0.001g of monomer cannot be dissolved in 1 mL of solvent. Similarly, the threshold for IPA (Fig. S7c, 7d) and MeOH (Fig. S7e, 7f) are between 500-1000 and 100-500, respectively. Thus, THF, IPA, and MeOH with increased polarities show very poor, poor, and limited affinities towards monomer SBMA, respectively.

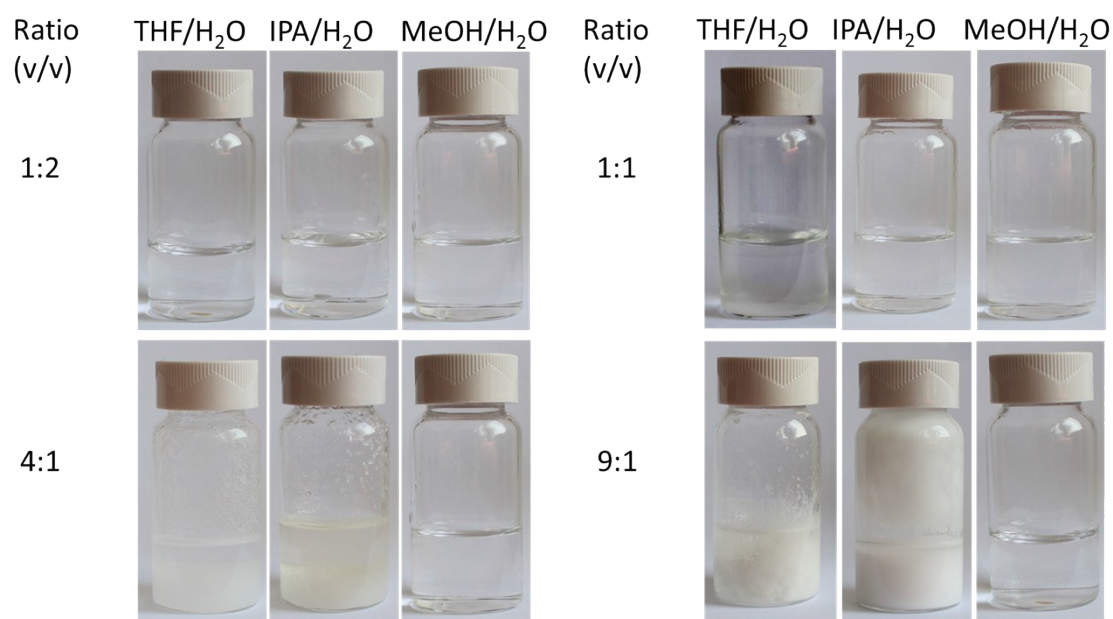


**Fig. S8** Images of zwitterionic monomer SBMA dissolving in various binary solvents.

The affinity of zwitterionic monomer towards organic solvent can be further identified from its solubility in mixed solution. As we all know that water is miscible to THF, IPA, and MeOH at various ratios. However, this phenomenon was changed significantly when the zwitterionic monomer SBMA was introduced. From Fig. S8, it can be seen that all binary solvents were capable of dissolving monomer SBMA well at low ratio of organic solvent compared to water (e.g. 1:2). For THF and water mixture, there appeared two layers when the ratio between water and THF decreased to 1:1, while the other two solvents were good for dissolving. The separated top layer was THF due to its lower density than water, indicating the poor affinity of THF towards water containing zwitterionic monomer molecules. With the decrease of water volume, e.g. 4:1, the IPA and water binary solution became cloudy. However, a clear solution was observed even at a ratio of 9:1 for methanol and water system. These results clearly demonstrate that THF, IPA, and methanol has poor, moderate, and good affinity towards water combined zwitterionic monomer molecules, respectively.

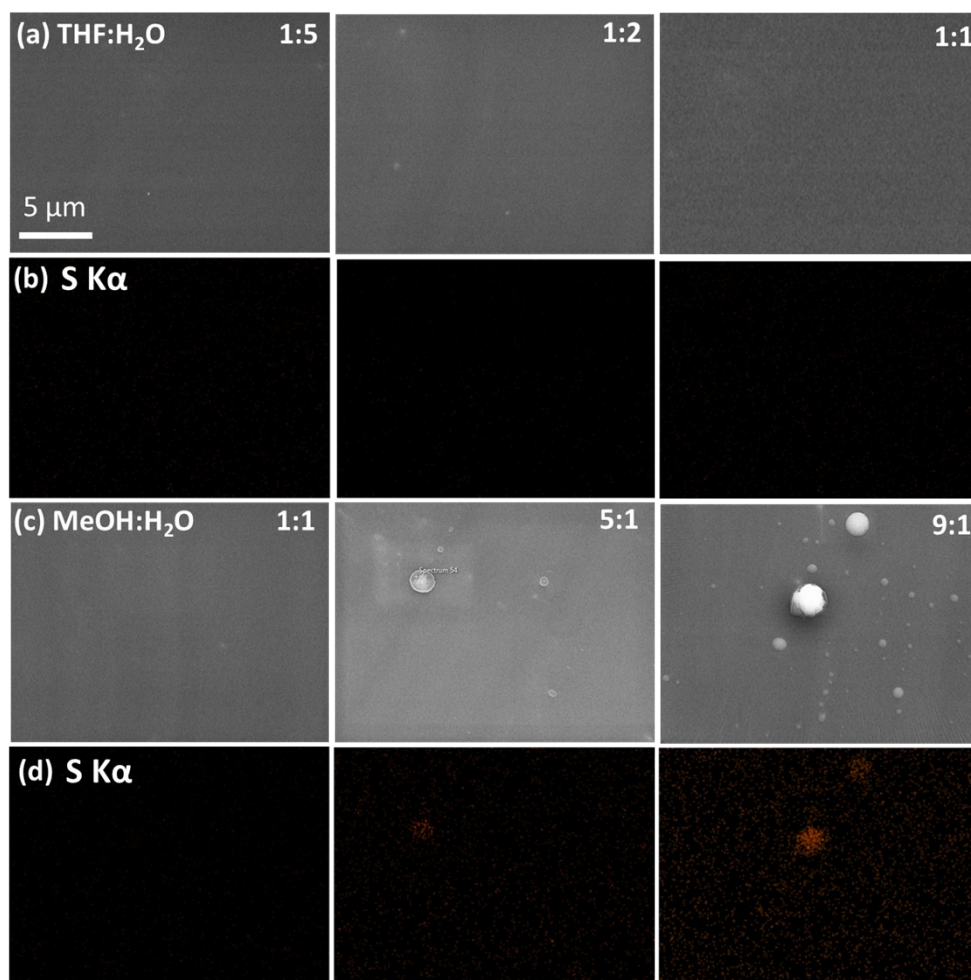


**Fig. S9** SEM images and EDX atom S mapping of (a, b) THF:H<sub>2</sub>O and (c, d) MeOH:H<sub>2</sub>O at different ratios.

For case of THF binary solvents, subsurface morphology of PDMS surface (~1 mm depth) was clear (Fig. S9a) and no sulphur element was observed (Fig. S9b), regardless of the ratio between THF and water. Regarding to MeOH binary solvents (Fig. S9c, 9d), a clear surface and no sulphur element was detected when MeOH:H<sub>2</sub>O was 1:1. However, several small particles associated with tiny sulphur element were identified when the ratio was 5. With the increase of ratio, the number of particles and sulphur element was increased.

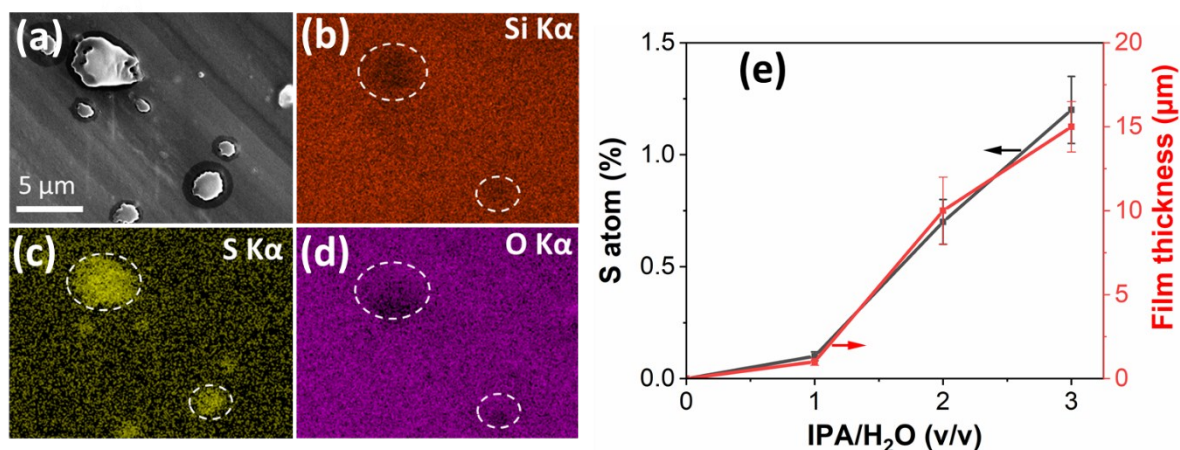


**Fig. S10** (a-d) SEM image (IPA: H<sub>2</sub>O=2:1) and its corresponding EDX mapping. (e) S atom percentage and film thickness at different ratios of IPA and water.

For IPA binary solvent (IPA:H<sub>2</sub>O=2:1), several irregular blocks were identified (Fig. S10a) and they should be monomer SBMA, because it is in that area where the silicon element is absent (Fig. S10b) while sulphur (Fig. S10c) and oxygen elements (Fig. S10d) are present. In addition, Fig. S10e shows the dependence of atom percentage of sulphur on the ratio of IPA to water, which is consistent with the change in film thickness.

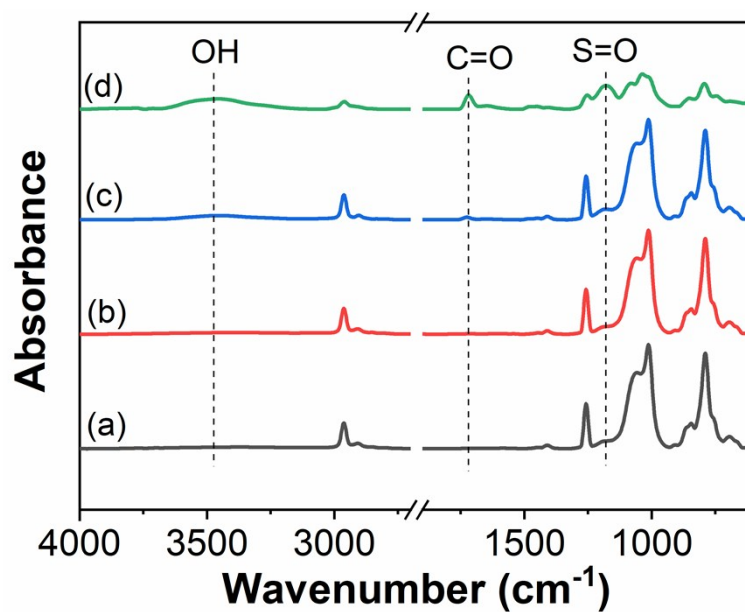


**Fig. S11** ATR-FTIR spectra of (a) iPDMS and PSPMA-grafted iPDMS when using water-organic binary solvents: (b) THF; (c) MeOH; (d) IPA.

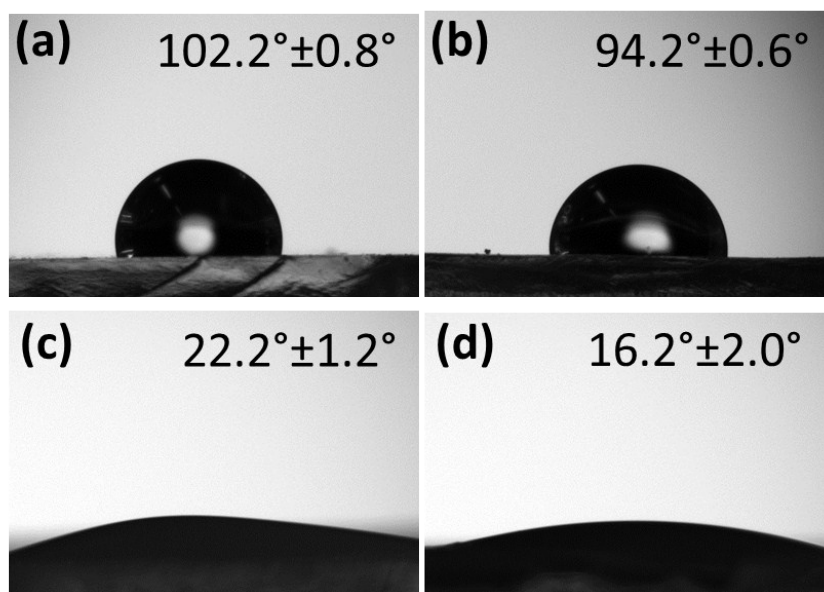


**Fig. S12** Water contact angle of (a) iPDMS and PSPMA-grafted iPDMS when using water-organic binary solvents: (b) THF; (c) MeOH; (d) IPA.

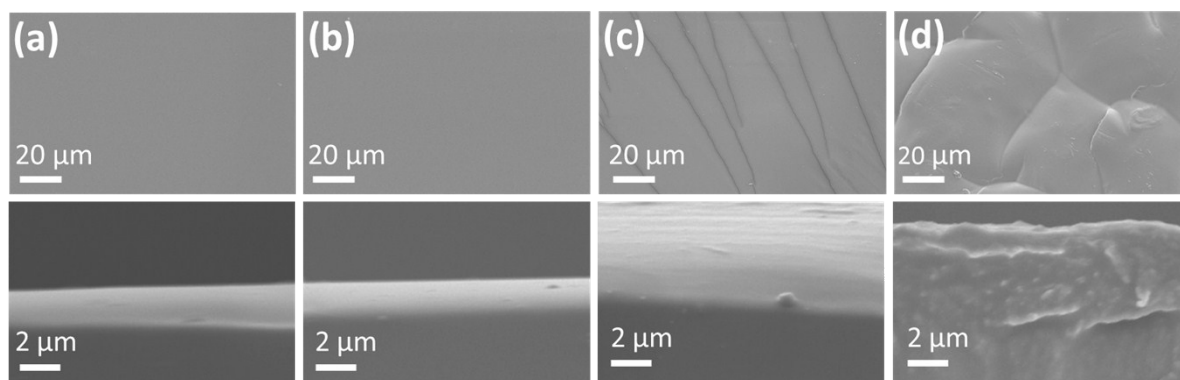


**Fig. S13** SEM images of (a) iPDMS, and PSPMA-grafted iPDMS when using water-organic binary solvents: (b) THF; (c) MeOH; (d) IPA.

## References

1. K. Matyjaszewski, S. G. Gaynor, A. Kulfan and M. Podwika, *Macromolecules*, 1997, **30**, 5192.
2. K. Matyjaszewski, S. G. Gaynor and A. H. Müller, *Macromolecules*, 1997, **30**, 7034.
3. L. Y. Yeo, H. C. Chang, P. P. Chan and J. R. Friend, *Small*, 2011, **7**, 12.
4. Q. Fu, H. Zhang, Z. Wang and M. J. Chiao, *J. Mater. Chem. B*, 2017, **5**, 4025.
5. I. Johnston, D. McCluskey, C. Tan and M. C. Tracey, *J. Micromech. Microeng.*, 2014, **24**, 035017.
6. M. Liu, J. Sun and Q. Chen, *Sens. Actuator A Phys.*, 2009, **151**, 42.
7. Z. W. Tang, C. Y. Ma, H. X. Wu, L. Tan, J. Y. Xiao, R. X. Zhuo and C. J. Liu, *Prog. Org. Coat.*, 2016, **97**, 277.
8. X. Sui, Q. Chen, M. A. Hempenius and G. J. Vancso, *small*, 2011, **7**, 1440.
9. W. Yoshida and Y. Cohen, *J. Membr. Sci.*, 2003, **215**, 249.
10. P. Schön, E. Kutnyanszky, B. T. Donkelaar, M. G. Santonicola, T. Tecim, N. Aldred, A. S. Clare and G. J. Vancso, *Colloids. Surf. B*, 2013, **102**, 923.
11. D. M. Davenport, J. Lee and M. Elimelech, *Sep. Purif. Technol.*, 2017, **189**, 389.
12. H. Ma, D. Li, X. Sheng, B. Zhao and A. Chilkoti, *Langmuir*, 2006, **22**, 3751.
13. E. Rogers and I. Stovall, *Fundamental of chemistry: Solubility*, New York, Department of Chemistry. University of Wisconsin, 2000.